Angel Garcia-Martino[1], Santos Fernández[2], Jesús Santiago[3], Maria Manuela Prieto[4]

[1] *Finishing & Product Technologies, Global R&D ArcelorMittal,*

Av. Marqués de Suances 33402 Avilés, Spain

[2] *Quality Department, Operation Finishing ArcelorMittal Asturias,*

Trasona, s/n, 33400 Avilés, Spain

[3] *Technical Department, Operation Finishing ArcelorMittal Asturias,*

Trasona, s/n, 33400 Avilés, Spain

[4] *Energy Department, Universidad de Oviedo,*

East Building, Campus of Gijón, Wifredo Ricart, s/n,

33204 Gijón, Spain

The consequences of eliminating the soaking Section of a commercial hot-dip galvanising line for HSLA production and a control strategy for improving product consistency

This paper describes the results of the investigations done to adapt the thermal cycles applied to High Strength Low Alloy (HSLA) steels to the new furnace configuration of a galvanizing line. During the revamping of a hot dip galvanizing line, new radiant tubes were installed in the soaking furnace with the purpose of increasing the line capacity. This modification eliminated the soaking stage and forced to redesign the thermal cycles of the furnace. As the classical cycles proposed for the HSLAs worrisomely increased the percentage of rejections, it was defined a new control parameter based on the strip thickness, time in the furnace and strip temperature to guarantee the mechanical characteristics of these steels.

Keywords: HSLA, galvanizing, soaking, annealing, time, process window, mechanical characteristics, thermal cycle redesign

Nomenclature

S_{fcl}	curve speed at furnace capacity limit for a given thickness
E	difference S-S^* in eq. (7)
El	elongation (%)
S	curve of speed for a determinate value T-t (m/min)
S^*	curve of speed for a determinate value T-t in eq. (6)
S_{upper}	Value of the strip speed corresponding to the Intersection of the line T-t max with the target temperature at the exit of the furnace (P3) (m/min)
S_{lower}	Value of the strip speed corresponding to the intersection of the line T-t min with the target temperature at the exit of the furnace (P3) (m/min)
T	temperature (ºC)
T-t	time-temperature parameter
UTS	ultimate tensile strength (MPa)
WP	working point
YS	yield strength (MPa)

Subscripts

coil –i	each one of the coils used to calculate the T-t limits
fcl	curve of the limit capacity of the furnace for a given thickness
max	value of speed in the curve T-t min
min	value of speed in the curve T-t max
th	strip thickness

Subscripts

c	curve calculated with a quadratic correlation approach

Introduction

High Strength Low Alloyed (HSLA) steels are designed to meet specific mechanical properties rather than a chemical composition, thus are not considered alloy steels in the normal sense [1-3].

If we focus on galvanized product, despite the development of the different generations of Advanced High Strength Steels (AHSS) [4], HSLA are still commonly used for the body-in-white parts of the automotive industry. The composition and technical characteristics of the ordinary HSLA grades, all of them offered by ArcelorMittal [5], are shown in Table 1 and Table 2. The microalloying elements used to increase the strength are Vanadium, Titanium and Niobium in different percentages depending on the HSLA grade.

In case of HSLA steels produced in a hot dip galvanizing (HDG) line, the achievement of the required mechanical properties will depend on the chemical composition, finish rolling temperature, cold rolling reduction and thermal cycle applied [6-8].

The classical thermal cycle in a HDG line has four stages: heating, soaking, cooling and overaging. The most important parameter to be defined is the target temperature at the end of the heating section, which remains stable during the soaking. As it is not possible to guarantee the exact temperature due to the complexity of the process, a given margin around this target temperature is allowed, which could be wider or narrower depending on the product requirements. Other parameters to be taken into account are the temperatures during the cooling phase and the Zn-bath entry temperature.

This paper describes the problem that arose with mechanical characteristics of HSLAs after the soaking stage elimination in a radiant tubes furnace, and the definition and utilization of a new process control parameter to solve the problem.

Case study

The furnace of an ArcelorMittal HDG line was revamped to increase its productivity with the installation of additional radiant tubes in the soaking chamber. This improvement made possible an additional strip heating when it passes through the soaking section. Thus, the new thermal cycles have only three stages: heating, cooling and overaging. This new configuration led to the redesign of the thermal cycles for all range of steels produced, including HSLA steels. Figure 1 shows the thermal cycle redesign, comparing the classic cycle with soaking and control in P2 versus the new cycle without soaking and control in P3.

The lack of historical data with this new configuration prevented the design of the new thermal cycles using data-driven models [9], thus the migration was progressive: for each cycle, first it was made an adjustment using simulations tools and lab tests with the Rhesca ® galvanizing simulator, then every new cycle had to be checked during one or more scheduled trials in the line before to be approved for its industrial use.

However, problems with the cycles designed for HSLA were found in the industrialization phase, and the line suffered a severe crisis of quality. The percentage of internally rejected coils due to mechanical characteristics raised worrisome achieving values between 6% and 16% of rejections depending on HSLA steel grade. As example, in Figure 2 are shown the results of the tensile tests after the application of the new cycles without annealing for the HSLA340, which was the most affected by the mechanical characteristics scattering. The distribution of these rejections was heterogeneous, having heavy impact in some strip thicknesses meanwhile others were produced within the normal quality ratios. The rejection rate evolution for HSLAs after the application of the new cycles without soaking is shown in Figure 3.

Since there had been no changes in the upstream processes, the analysis focused on the galvanizing process. Initially it was suggested that the problem could be related to the higher target temperature of the new cycles, but this would have caused a decrease of the yield strength values [10]. This hypothesis was finally discarded because they were found also a lot of coils with the yield strength over the maximum limit. This increase matches with the result of reducing the annealing time [11] due to the general increase of the speed obtained after the revamping, so it pointed to a combined time/temperature effect on the annealing and recrystallization processes [12] and its consequences on the phase transformation [13]. It was also studied if other process parameters such as the chemical composition, the coiling temperature at the hot rolling mill [10] or the cold rolling reduction ratio [12] could explain the strong influence of strip thickness on the final results, but even though this influence is clear, it could not be found in the process

data a relevant correlation which could help to solve the problem and be able to diminish the rejections.

In addition, there was still a need to define a new parameter to improve the control of the process. The possibility to keep the old thermal cycles with soaking for the HSLA and the new ones (without it) for the rest of the steel grades was immediately discarded, as it would lead to thermal transitions involving different control pyrometers. These transitions would have a big impact in the productivity of the line and also in the quality results, because the thermal inertia of the furnace makes that the material produced during the transition may be out of the required mechanical characteristics [14, 15, 16, 17].

Conceptual approach

Faced with the difficulty of defining a thermal cycle in a classical way, and it being evident that the elimination of the soaking stage was affecting the results of HSLAs, a new restriction in the cycle was described: the T-t parameter.

The T-t parameter is defined to ensure a minimum of energy is absorbed by the strip once the recrystallization starts. For the calculation of this parameter it was necessary to use an in house developed furnace heating model that calculates not only the target temperature but also the heating profile of the strip along the furnace.

As it is depicted in Figure 4, the T-t parameter (5) is defined as the area defined by the strip thermal profile (1) and the recrystallization temperature (2). To determinate the value of the upper and lower limits for T-t parameter, the population of HSLA coils produced in that period of time was studied. It can be observed in Figure 2 that scattering is higher for yield strength (YS) than for ultimate tensile strength (UTS), therefore the definition of T-t limits was based on YS results to obtain more restrictive values and avoid coil rejections.

Using the in house developed heating model, the T-t parameter for each coil whose test result was close to YS_{max} or YS_{min} values was calculated. The definitive T-t_{min} and T-t_{max} limits were defined respectively as the maximum and minimum values obtained:

$$YS_{Coil-i} \cong YS_{max} \rightarrow T - t_{min} = Max(T - t_{Coil-i})$$
$$YS_{Coil-i} \cong YS_{min} \rightarrow T - t_{max} = Min(T - t_{Coil-i})$$

These maximum and minimum T-t values represented a new restriction to be taken into account for the definition of the thermal cycles. Figure 5 shows graphically how the application of the T-t parameter to the thermal cycles design implied a change of philosophy: instead of the classical definition pointing to a fixed target temperature plus/minus a given offset, different combinations of temperature and speed were defined to fulfill the T-t_{max} and T-t_{min} values.

The heating model was updated to calculate the process set-ups that meet the predefined requirement for the T-t parameter. being obtained an area as shown in Figure 5. The Process Window being defined as the region within the feasibility area of the line limited on the right by the heating capacity of the furnace, and above and below by the curves defined by temperature-speed pairs corresponding to T-t_{max} and T-t_{min} limits. From the Process Window shape, it can be deducted that the temperature is more restrictive than the time [18] to obtain the desired characteristics, since the range of feasible speeds

for a given working point (WP) is wider than for temperatures. It is also observed that the lower is the temperature the longer annealing time is required.

Figure 6 presents the Process Window corresponding to two thicknesses X and Y, being Y fifty percent thicker than X. As there is not a common range of temperatures valid for all the process windows, it is not possible to define a classical thermal cycle for the complete thicknesses range processed in the line. This also explained the heterogeneous distribution of the rejections experimented in the line: the overlapping between the classical thermal cycle definition and Process Window varies depending on the strip thickness.

Therefore, it was necessary to modify the control of the furnace to integrate this relationship between the target temperature and the speed, so that if the speed of the line decreased, the temperature would also be readjusted to keep the product within the range of mechanical characteristics required. Hence, to address the modification in the control, it was necessary first to define mathematically the Process Windows, thus obtaining the relation between the two process parameters (speed and temperature) according the strip thickness.

Mathematical Development

Figure 7 shows the strip speed values S_{lower} and S_{upper}, defined as the intersection of the curves T-t_{max} and T-t_{min} with the curve of maximum capacity of the furnace, for the complete range of thickness produced discretized in 0.1 mm increments.

A linear correlation between speed (S) and temperature (T) is obtained.

$$S_{upper} = A_{upper} \cdot T + B_{upper} \quad (1)$$

$$S_{lower} = A_{lower} \cdot T + B_{lower} \quad (2)$$

Before analyzing how to determine these A and B coefficients as function of the strip thickness, it is necessary to define the matrix representation of the Process Window, shown in Figure 8. The column 1 is the range of target temperatures. The columns 2 and 3 correspond to the minimum and maximum speeds given by the intersection of the temperature with the T-t_{max} and T-t_{min}, limits respectively. Finally, the column 4 is the value of the speed given by the intersection of the temperature with the furnace capacity curve between S_{lower} and S_{upper} (see Figure 5). Taking increments of 5º C, a 32 x 4 matrix is obtained for each thickness.

From this point, columns 2, 3 and 4 of the matrix are taken as independent vectors.

$$S_{min} = [S_{min,1}\ ,\ S_{min,2}\ , \cdots , S_{min,31}] \quad (3)$$

$$S_{max} = [S_{max,1},\ S_{max,2}, \cdots\ ,\ S_{max,31}] \quad (4)$$

$$S_{fcl} = [S_{fcl,1},\ S_{fcl,2}, \cdots,\ S_{fcl,31}] \quad (5)$$

As the procedure developed is the same for S_{min}, S_{max} and S_{fcl}, only S_{min} calculations will be shown in detail. The first step is to calculate a new S^{*}_{min} vector, whose elements are determined with the corresponding correlation (2).

$$S^{*}_{min} = \left[S^{*}_{min,1},\ S^{*}_{min,2}, \cdots, S^{*}_{min,31}\right] \quad (6)$$

$$\forall S^{*}_{min\_i} \neq 0 \ \rightarrow S^{*}_{min,i} = A_{lower} \cdot T_i + B_{lower}$$

The vector E^{*}_{min} defined as the difference between S_{min} and S^{*}_{min} gives an idea of the error arising from using this correlation, which is in this first approximation is high.

$$E^{*}_{min} = S_{min} - S^{*}_{min} \quad \forall \left|E^{*}_{min,i}\right| \uparrow\uparrow \quad (7)$$

It is observed that, the lower is the speed, the higher is the error, due to the fact that these points are further from the speed values used for establishing the correlation (2). In order to reduce this error, the correlation existing between the different $E^{*}_{min,i} \neq 0$ is studied.

Figure 9 shows the representation of the error values obtained for determinate thicknesses when a quadratic correlation is proposed, however the results regarding the adjustment of the quadratic correlation can be extended to the rest of them.

As it was done in (6), the S^{C}_{min} vector is calculated using this new correlation:

$$S^{C}_{min} = \left[S^{C}_{min,1}, S^{C}_{min,2}, \cdots, S^{C}_{min,31}\right] \quad (8)$$

$$\forall S^{C}_{min,i} \neq 0 \ \rightarrow S^{C}_{min,i} = a \cdot T_i^2 + b \cdot T_i + c$$

The procedure continues comparing the values calculated with this new vector with original one, by defining the error vectors as was done in (7), but in this case the error, whatever the thickness, is very low:

$$E^{C}_{min} = S_{min} - S^{C}_{min} \quad \forall \left|E^{C}_{min,i}\right| < 2 \quad (9)$$

Similar result, in terms of very low error, is obtained when E^{C}_{max} is calculated. In this way, the relation of speed and temperature for each thickness (th) is defined as:

$$S_{min,i,th} = a_{min,th} \cdot T_i^2 + b_{min,th} \cdot T_i + c_{\ min,th} \quad (10)$$

$$S_{max,i,th} = a_{max,th} \cdot T_i^2 + b_{max,th} \cdot T_i + c_{max,th} \quad (11)$$

The last step is to establish the relation between the coefficients as function of the thickness, in order to obtain a final general expression. Taking increments of 0.1 mm, fourteen cases can be defined. Figure 10 shows the results of plotting the values of the coefficients $a_{min,th}$, $b_{min,th}$ and $c_{min,th}$:

From Figure 10 is depicted the possibility of describing the coefficients obtained in (10) as function of the strip thickness, obtaining in this way a general expression for all the combinations of speed, temperature and thickness:

$$A = \ coef_1^a \cdot th^2 + coef_2^a \cdot th + coef_3^a \quad (12)$$

$$B = \text{coef}_1^b \cdot th^2 + \text{coef}_2^b \cdot th + \text{coef}_3^b \qquad (13)$$

$$C = \text{coef}_1^c \cdot th^2 + \text{coef}_2^c \cdot th + \text{coef}_3^c \qquad (14)$$

And substituting in (10), the final general expression it is obtained:

$$S_{min,i} = A \cdot T_i^2 + B \cdot T_i + C \qquad (15)$$

Where the coefficients A, B y C according to formulae (12 to 14) can be written as:

$$A = \sum_1^3 \text{coef}_i^a \cdot th^{3-i} \quad B = \sum_1^3 \text{coef}_i^b \cdot th^{3-i} \quad C = \sum_1^3 \text{coef}_i^c \cdot th^{3-i}$$

Results

The implementation of this control parameter led to an immediate improvement in the quality results, not only due to a better process control, but also because the T-t parameter proved to be very useful for the on-line product control. Figure 11 shows the skin-pass rolling force for a fixed elongation target and the T-t parameter along a HSLA coil. It is clearly shown that the variation in the T-t values (due to transient in the furnace) leads to hardness evolution in the material which is reflected in the skin-pass force behavior and confirmed by physical testing too. This fact enabled the definition of quality blocking rules, based on T-t along the coil, to detect and remove material out of specification, mainly associated with difficult transitions, unforeseen speed drops and other process issues.

Since the new Process Windows were implemented in the middle of October 2011, the internal rejection ratio diminished from 5-16% to under 0.5% as is shown in Figure 12

In the next year, the rejection ratio in HSLA kept low (0.43%), similar to that obtained with soaking and control in P2 at lower speed, and this result has remained stable up to the present date.

Conclusions

A new control parameter to guarantee HSLAs mechanical characteristics produced without a soaking step was defined. The introduction of this parameter led to a redefinition of the thermal cycles for these steels. New Process Windows were set up, based on the combination of speed and target temperatures which complies with the maximum and minimum limits of the control parameter.

Process Windows for different HSLA grades were successfully integrated in the process. The rejection of coils due to non-compliant mechanical properties was greatly reduced and it has remained stable, with values below 0.5%, since their implementation.

Acknowledges

The authors greatly acknowledge ArcelorMittal for supporting this investigation and Avilés 2 line staff for their collaboration during the development of trials.

References

[1] Daviss JR. Alloying: Understanding the Basics. Materials Park (OH): ASM International, 2001; p. 193.

[2] Bhadeshia H, Honeycombe R. Steels: Microstructure and properties. Oxford: Elsevier, 2017.

[3] Skobir D. High-strengh low-alloy (HSLA) steels. Mater. and Technol. 2011; 45(4): 295-301.

[4] Bhattacharya D.Tecnologia em Metalurgia. Mater. e Min. 2014;11(4): 371-383

[5] High strength low alloy (HSLA) steels for cold forming [Internet]. ArcelorMittal 2017. Available from http://automotive.arcelormittal.com/europe/products/HYTSS/HSLA/EN.

[6] Bakkaloğlu A. Effect of processing parameters on the microstructure and properties of an Nb microalloyed steel. Mater. Lett. 2002; 56: 263-272.

[7] Gladman T. The physical metallurgy of microalloyed steels. London: Institute of Materials, 1997.

[8] Korczak P. Influence of controlled rolling condition on microstructure and mechanical properties of low carbon micro-alloyed steels. J. of Mater. Process. Technol. 2004; 157(58): 553-556.

[9] Sanz-García A, Fernández-Ceniceros J, Fernández-Martínez R, Martínez-de-Pisón J, Methodology based on genetic optimisation to develop overall parsimony models for predicting temperature settings on annealing furnace, Ironmaking & Steelmaking, 2014; 41(2): 87-98.

[10] Yashchuk S, Rodionova I, Zaitsev A et al. Effect of chemical composition and production parameters of hot rolling and recrystallization annealing in continuous hot dip galvanizing units on the structure and properties of high-strength low-alloy steels. Metallurgist. 2011; 54(9-10): 608-617.

[11] Raji NA, Oluwole OO. Effect of soaking time on the mechanical properties of annealed cold-drawn low carbon steel. Mater. Sci. and Appl. 2012;3:513-518.

[12] Janošec M, Schindler I, Vodárek V et al. Microstructure and mechanical properties of cold rolled, annealed HSLA strip steels. Arch. of Civ. and Mech. Eng. 2007;7(2):30-38.

[13] Hüysein A, Havv KZ, Ceylan K. Effect of intercritical annealing parameters on dual phase behaviour of commercial low-alloyed steels. J. of Iron and Steel Res, Intern. 2010;17(4): 73-78.

[14] Wu H, Speets R, Heeremans F, Ben Driss O, van Buren R. Non-linear model predictive control of troughput and strip temperature for continuous annealing line, Ironmaking & Steelmaking; 2015; 41(2): 87-98.

[15] Tottem GE, Funatani K, Xie L. Design of microstructures and properties of steel by hot and cold rolling. In Tottem GE, Funatani K, Xie L editors. Handbook of metallurgical process design. New York (NY): CRC Press; 2004. p 59-61.

[16] Taylor SW, Wang S. Overheating steel in an annealing furnace. ANZIAM 2010, Queenstown, New Zealand, 31 Jan 2010 - 04 Feb 2010. Am. Inst. of Phy. 2010; 1168: 1457-1460.

[17] Wu H, Speets R, Ozcan G, Ekhart R, Heijke R, Nederlof C, Boeder CJ, Non-linear model predictive control to improve transient production of a hot dip galvanising line, Ironmaking & Steelmaking. 2016; 43(7): 542-549.

[18] Huo X, Mao X, Lu S. Effect of annealing temperature on recrystallization behaviour of cold rolled Ti-Microalloyed steels. J. of Iron and Steel Res. 2013; 20(9):105-110.

Table 1 Chemical composition in %

Grade	C max	Mn max	Si max
HSLA 260	0.080	0.50	0.04
HSLA 300	0.080	0.60	0.04
HSLA 340	0.080	0.70	0.04
HSLA 380	0.080	0.90	0.35
HSLA 420	0.140	1.60	0.40

Table 2 Technical characteristics

Grade	YS	UTS	El
HSLA 260	260 – 320	350 – 410	≥ 28
HSLA 300	300 – 360	390 – 450	≥ 26
HSLA 340	340 – 400	420 – 490	≥ 23
HSLA 380	380 – 450	460 – 530	≥ 20
HSLA 420	420 – 520	470 – 590	≥ 17

Figure 1 Thermal cycle redesign and relocation of the control point

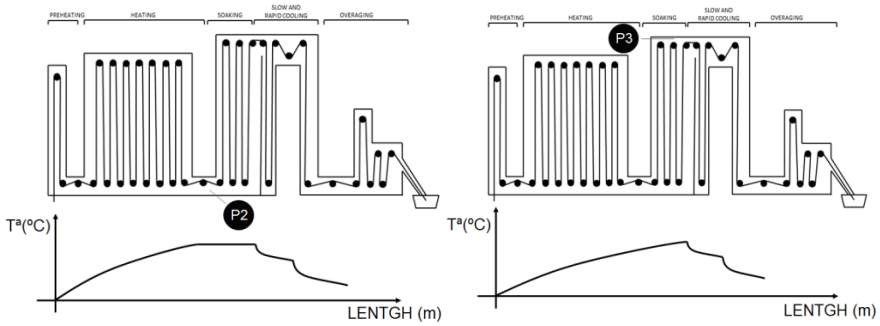

Figure 2 Tensile test results for HSLA340 grade

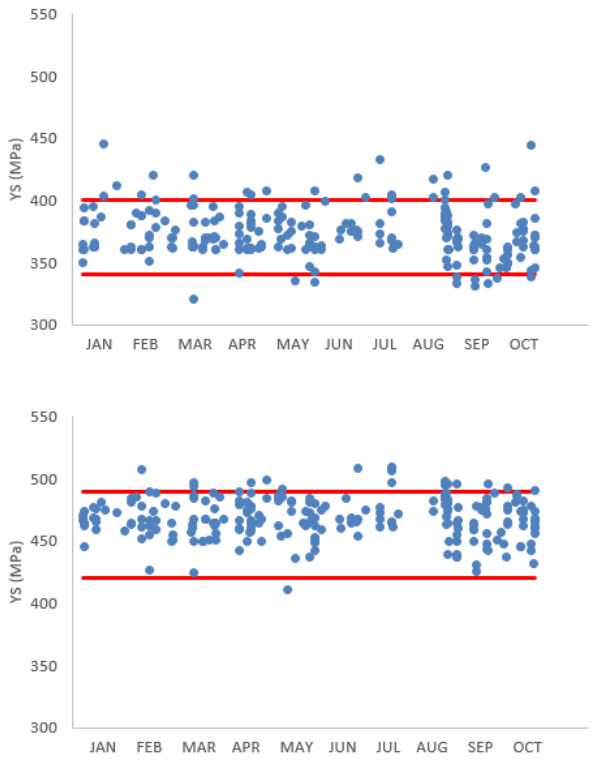

Figure 3 Evolution of rejections for HSLAs due to mechanical characteristics

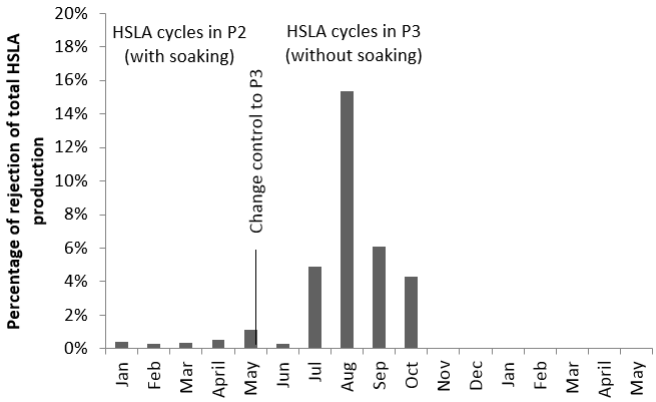

Figure 4 Definition of T-t parameter

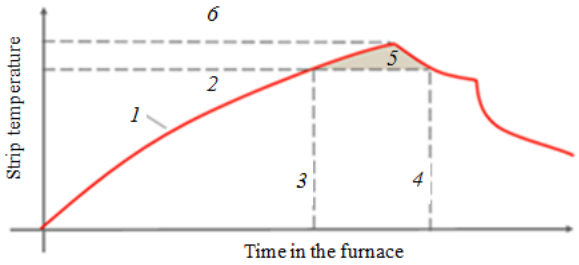

(1) Strip thermal profile

(2) Temperature of recrystallization

(3) to (4) – Time gap taken into account in the calculations

(5) T-t parameter

(6) Target temperature

Figure 5 Classical thermal cycle (above) vs Process Window (below)

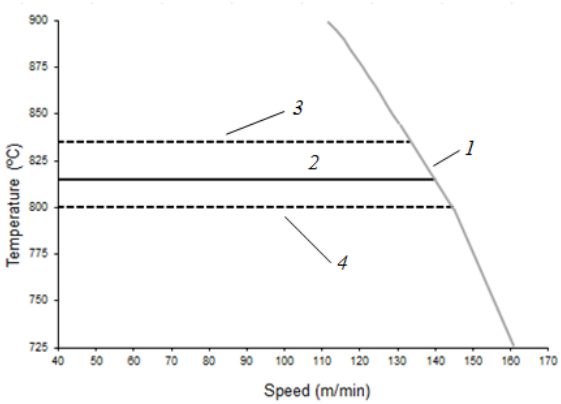

(1) Furnace capacity limit (2) Target temperature,
(3)Target temperature + offset 1 (4) Target temperature – offset 2

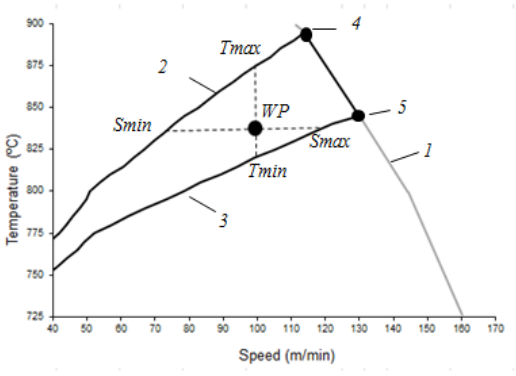

(1) Furnace capacity limit (2) T-tmax limit (3) T-tmin limit
(4) S_{lower} (5) S_{upper}

Figure 6 Process Windows calculated for different strip thickness of same steel grade

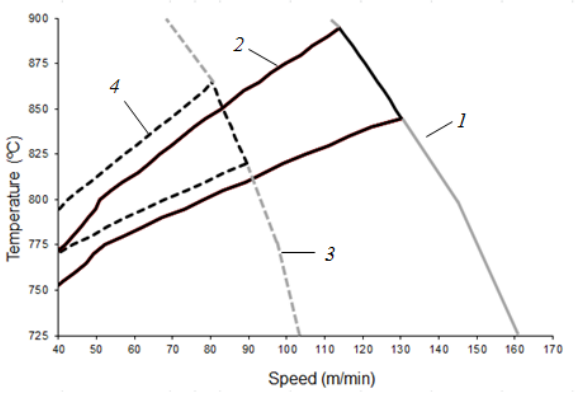

(1) Furnace capacity limit thickness X (2) Process Window for thickness X
(3) Furnace capacity limit thickness Y (4) Process Window for thickness Y

Figure 7 Correlation between maximum speeds

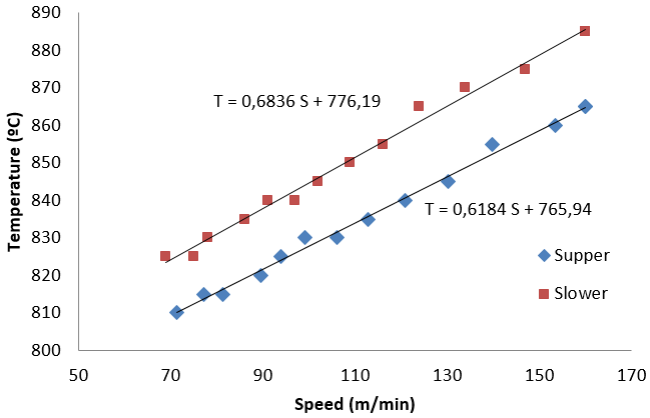

Figure 8 Matrix representation of the Process Window

Temperature (ºC)	*Speeds in T-t max limit*	*Speeds in T-t min limit*	*Speed for Furnace capacity limit*
T_0	$S_{min,0}$	$S_{max,0}$	$S_{fcl,0}$
T_1	$S_{min,1}$	$S_{max,1}$	$S_{fcl,1}$
T_2	$S_{min,2}$	$S_{max,2}$	$S_{fcl,2}$
⋮	⋮	⋮	⋮
T_{31}	$S_{min,31}$	$S_{max,31}$	$S_{fcl,31}$

Figure 9 Errors with quadratic adjustment

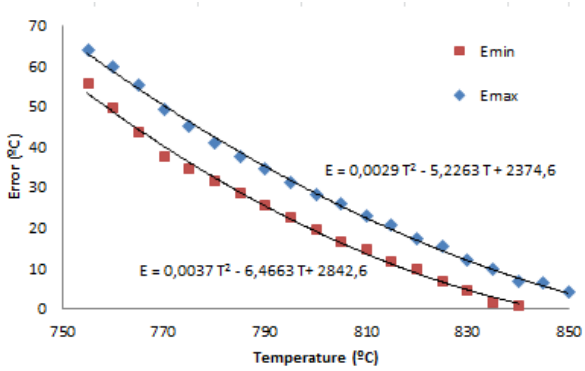

Figure 10 Correlation between the coefficients and strip thickness

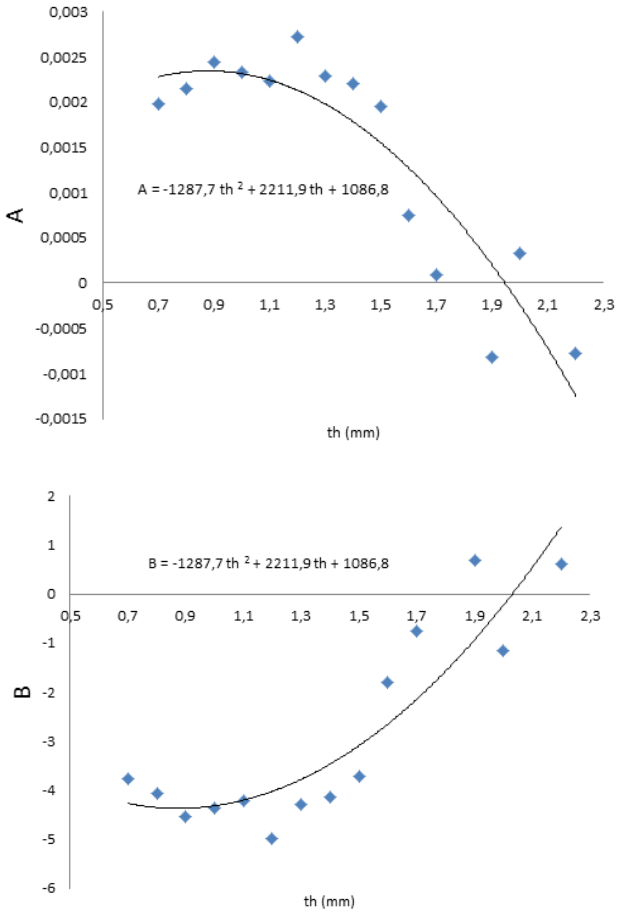

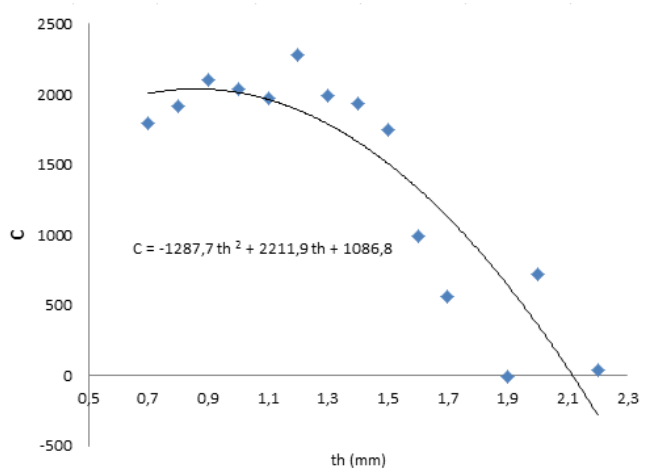

Figure 11 Skin-pass force vs T-t parameter

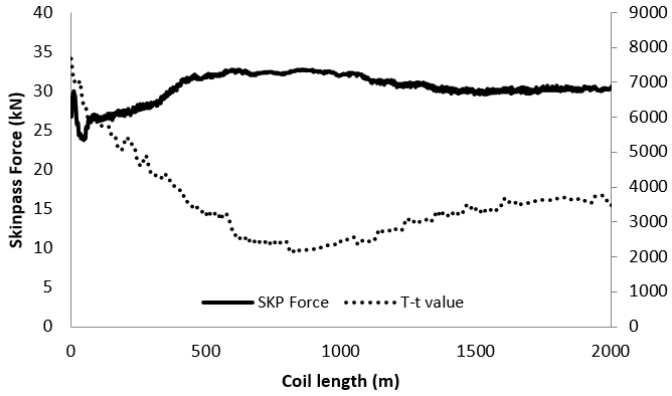

Figure 12 Evolution in internal rejection ratio using new Process Windows